NTU Journal of Engineering and Technology (ICSDT2025) special issue
DOI: https://doi.org/10.56286/ntujet.icsdt2025

IRAQI Academic Scientific Journals

P-ISSN: 2788-9971 E-ISSN: 2788-998X
NTU Journal of Engineering and Technology
Available online at: https://journals.ntu.edu.iq/index.php/NTU-JET/index

Performance of Partially Concrete Filled C-purlin Beam-Slab System: Numerical Investigation

Alyaa A. Al-Attar[1], Ahmed W. Al Zand[2], Mohammed Ch. Liejy[1], Azrul A. Mutalib[3], Idan I. Ghdhban[1]

[1]Northern Technical university, Kirkuk 36001, Iraq,
[2]Department of Design, College of Fine Arts, Al-Turath University, Baghdad, Iraq,
[3]Department of Civil Engineering, Universiti Kebangsaan Malaysia (UKM), 43600 Bangi, Selangor, Malaysia.

dr.alyaa@ntu.edu.iq, ahmed.zand@uoturath.edu.iq , mohammedchead_hwj@ntu.edu.iq , azrulaam@ukm.edu.my, idan_hwj@ntu.edu.iq

Article Informations

Received: 15-03- 2025,
Accepted: 28-04-2025,
Published online: 01-03-2026

Corresponding author:
Name: Ahmed W. Al Zand
Affiliation: Al-Turath University
Email: ahmed.zand@uoturath.edu.iq

Key Words:
Composite structure,
profile steel sheet,
dry board.

A B S T R A C T

Lightweight cold-formed steel beams are widely utilized in roofing systems. Recently, engineers have increasingly used concrete-filled cold-formed steel tube beams for flooring systems due to their sufficient structural performance. A system that uses cold-formed steel beam sections with dry-board profile steel sheet slab (CBPDS) system would cost less than the conventional I-steel beam-slab system, with less self-weight, it is considered one of the types of sustainable buildings. This study numerically investigated the structural performance of the newly suggested composite beam-slab (CBPDS) system. It was found that the partially filled C-purlin beam can significantly affect the system in the elastic and plastic ranges for the specimens (CBPDS-DF, CBPDS-DS, and CBPDS-S). The bending capacity of the specimens with varied beam configurations (CBPDS-DF, CBPDS-DS, and CBPDS-S) was decreased by about 50% when using a partially filled specimen from Le to Le/5. This happens because there is less concrete in the area that is only partially filled to help resist bending forces, which in turn will accelerate its failure.

1. Introduction

Constantly striving to develop new composite structural components that are less costly, durable, ecologically friendly, and simpler to manufacture than conventional elements is the building sector. Many studies over the past thirty years have concentrated on investigating the performance of cold-formed profile steel sheets (PSS) coated with dry board (DB) sheets in lightweight composite slab systems [1–4], Often referred to as the PSSDB or PDS slab system. A superior binding contact between components of the PSS and the DB has been established utilizing self-tapping screws, which have been thoroughly examined through multiple direct push-out tests [5–7] Recently, numerous researches have examined the structural performance of the PSS slab system [8–11] and wall system [12–14] when integrated with concrete materials. Moreover, Al-Shaikhli et al. [9,10] examined, using the two-way slab concept, the bending behaviour of concrete-filled PSSDB slabs. Nevertheless, PSSDB deck slabs concrete or not usually have a shallow cross-sectional depth, which increases their susceptibility to notable deflection failure under normal static loads, which means they can be only used over a limited spanning length. Therefore, to carry a heavier load and/or adapt to a long span, concrete-filled PSSDB slabs must be supported by a beam, similar to the I-steel beam–slab concept [15–18]. Recently, Liejy et al.[19] investigated the effects of combining these two structural members in a single composite beam-slab system (CBPDS system), where they studied the influence of using normal concrete and recycled concrete as infill material with additional analytical and theoretical investigation for this type of composite system [19,20]. Therefore, this parametric study aims to examine the effects of different partially filled concrete (Le, Le/3, Le/4, and Le/5 of C-purlin beam lengths) on the behaviour of the CBPDS system using numerical modeling and compare it with experimental specimens in [19]. Based on that. Twelve (12) FE models of double-filled, separate, and single specimens (CBPDS-DF, CBPDS-DS, and CBPDS-S) are developed and analyzed using ABAQOUS software to investigate further parameters that are not experimentally tested.

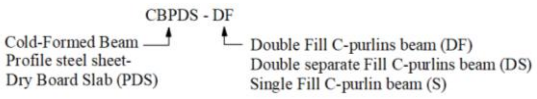

Fig. 1. Specimens designation ID.

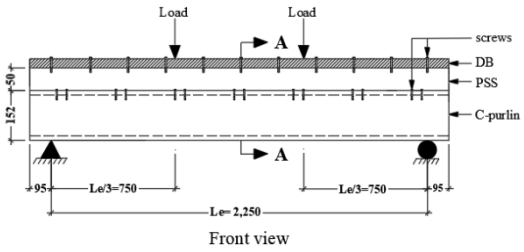

Front view

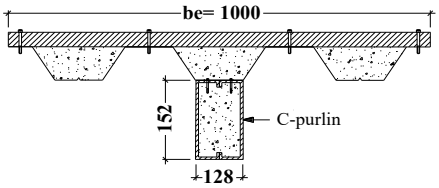

a) Section A-A Double Fill beam (CBPDS-DF)

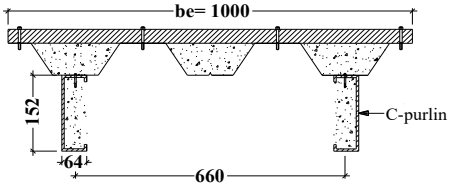

b) Section A-A Double Separate Fill beam (CBPDS-DS)

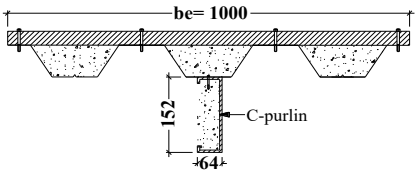

c) Section A-A Single Fill beam (CBPDS-S)

Fig. 2. composite CBPDS Specimens (EX).

2. Experimental Approcah

Composite CBPDS specimens are prepared in this research that is mainly fabricated from cold-formed-purlin beam (CB)and profile steel sheet-dry board (PSSB/PDS) deck slab, in which both parts of the beam and slab are filled with concrete material. For specimens, each C-purlin section is fabricated with 152 mm depth, 64 mm flange width, 16 mm lips length, and 2 mm thickness. The PSS section is fabricated with 1,000 mm width, 50 mm depth, and 1 mm thickness which are named Peva 50 (in the local market), which are covered by a dry board (DB) cement sheet (type Primaflex) with 1,000 mm width and 18 mm thickness. For easy and fast preparation of the suggested composite CBPDS system, all parts (DB with PSS and PSS with CB) are connected by self-tapping steel screws.

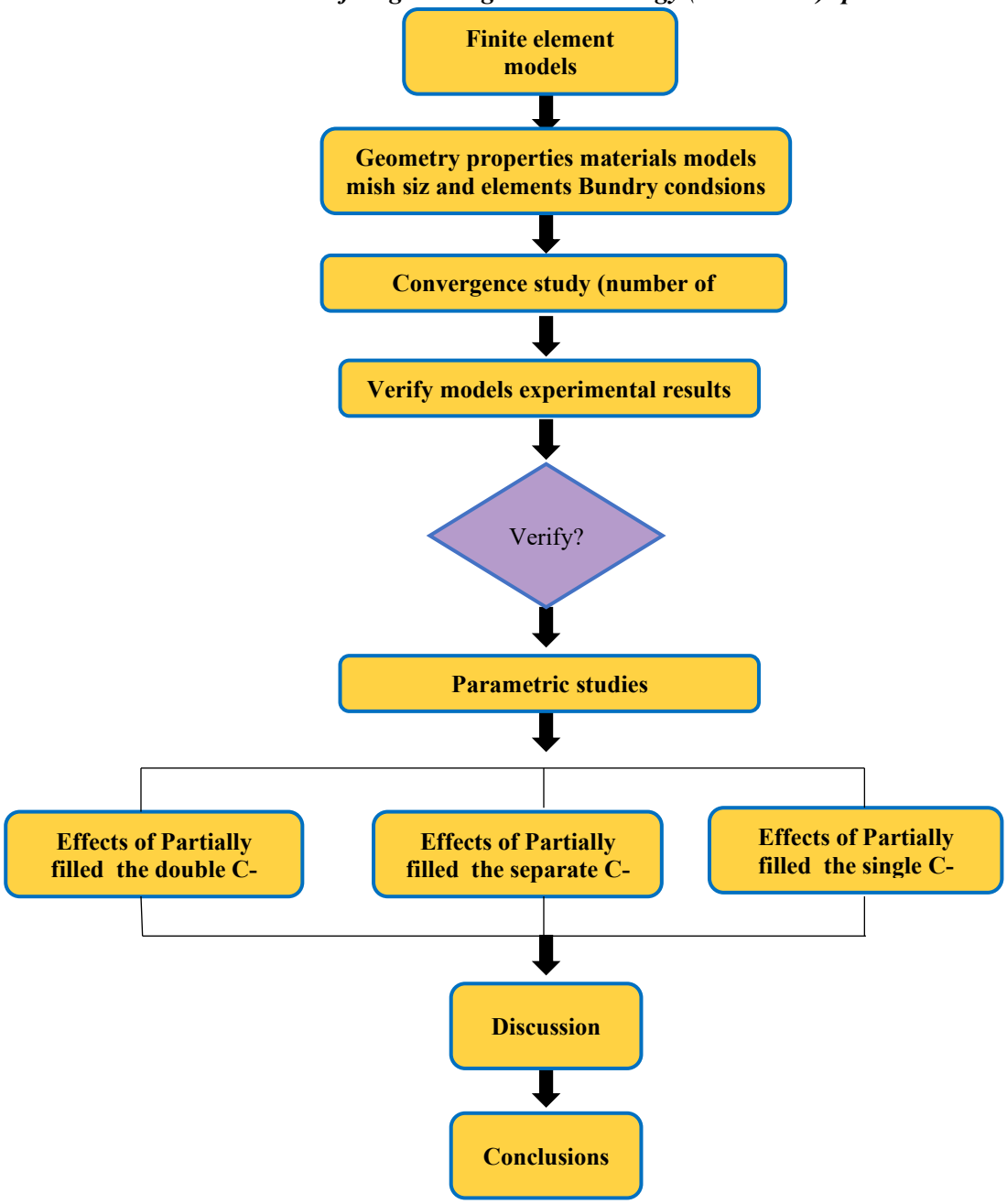

Fig. 3. Flow chart presenting the procedure of the current research.

The overall length of this specimens is equal to 2,440mm and the effective length (Le) are equal is to 2,250 mm [19].

Fig. 1 depicts the specimens designation ID. Fig. 2 present the detail of CBPDS specimens. The detail of specimens is presented in Table 1. Fig. 3 Flow chart presenting the procedure of the current research.

3. Finite Element Investigation

This paper reports the procedures of creating One nonlinear FE model based on the experimental specimen (double filled CBPDS-DF, DS, and S). ABAQUS/CAE FE software generated and analyses these FE models.

Modelling the structural components of this specimen was discussed in detail, including their material properties, loading methods, boundary conditions, and surface interactions. Fig.3 explains a flow chart that presents the procedure of this research. Therefore, the symmetrical method implemented in the ABAQUS software was utilized to generate the three-dimensional half models, which enabled a streamlined analysis on the personal computer (PC) see Fig 4. After verifying the suggested FE models with the existing experimental results, an additional 12 models were used in several parametric studies to further investigate the CBPDS-DF, CBPDS-DS, and CBPDS-S specimens' performance

Table 1. Physical properties of materials.

Materials	Dimensions Mm	Modulus of Elasticity (GPa)	Yield Strength (MPa)	Ultimate Strength (MPa)
Dry board (Primaflex)	**1,000x18**	**8.03**	**-**	**22**
Profiled Steel Sheeting (Peva 50)	**1,000 x1**	**213**	**434**	**464**
C-purlin	**152x64x2**	**210**	**492**	**536**

3.1. Element description

In order to obtain an accurate prediction of the behavior of the CBPDS system, it is critical to exercise great care in selecting the proper type for each component from the vast multitude of elements in the ABAQUS library. A shell element was chosen for the modeling of the PSS, DB, and C-purlin on account of their comparatively modest thickness when compared to other dimensions. ABAQUS provides two distinct varieties of shells, namely continuum shells and conventional shells.

The SR4 shell element, which is illustrated in Fig. 5, was selected for this research. This element has been effectively utilized by previous researchers [21–23] who have established their capacity to accurately predict the behavior of the PSS, C-purlin, and DB. The first-order hexahedral element (C3D8R) was employed to represent the infill concrete in this investigation, incorporating reduced integration and hourglass control (see Figure 5).

3.2. Material description

The materials included in the numerical analysis were steel (for the PSS, C-purlin, and DB) and concrete (for the infill). The properties of these materials were presented as follow:

The SR4 shell element, which is illustrated in Fig. 5, was selected for this research. This element has been effectively utilized by previous researchers [21–23] who have established their capacity to accurately predict the behavior of the PSS, C-purlin, and DB. The first-order hexahedral element (C3D8R) was employed to represent the infill concrete in this investigation, incorporating reduced integration and hourglass control (see Figure 5).

3.2.1. Concrete

Two different failure modes of concrete are crushing under compression and fracture under tension. The 'Concrete Damage Plasticity' function of the ABAQUS software is intended to characterize the 'Compressive Behaviour' and 'Tensile Behaviour' of concrete material in an independent manner.

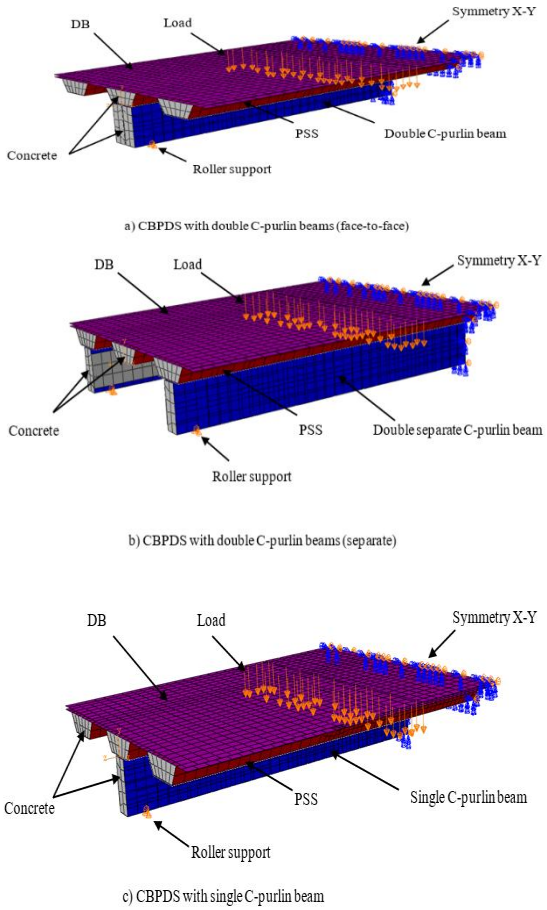

Fig. 4. 3D-half CBPDS finite element models (DF, DS, S).

Recent Finite Element (FE) investigations that examined the behavior of reinforcement concrete have successfully utilized this methodology, as evidenced by the works of [24–26]. It is noteworthy that concrete demonstrates isotropic characteristics within the elastic region, which prompted the 'Elastic-Isotropic' option to be chosen when computing Young's modulus and Poisson's ratio of the material. In order to account for the distinct strength and failure mechanisms in concrete under tension and compression, separate uniaxial stress-strain equations were utilized for these two conditions.

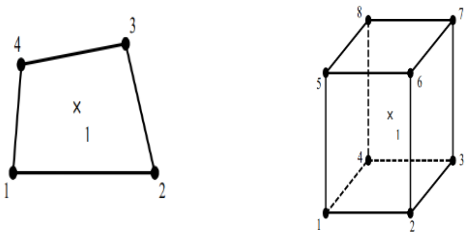

(a) S4R element (for steel and DB parts)

(b) C3D8R (for concrete part)

Fig. 5. Types of elements used in FE models.

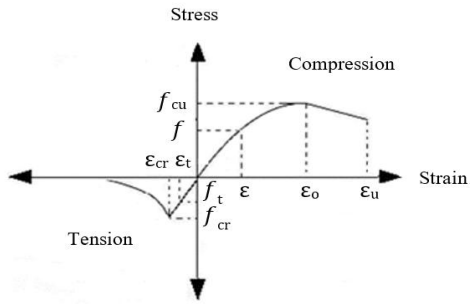

Fig. 6. Stress-strain curve for the concrete in the FE model [23].

Numerous equations have been put forth in past studies to represent these correlations, as described by [27–30] The constitutive uniaxial stress-strain curve for compressed concrete was employed in this study. The curve illustrated in Fig. 6 was obtained through the implementation of the numerical expression that (Bangash 1989) further refined after [27] work. This curve demonstrates linear elastic behavior for an estimated 30% of the ultimate compressive strength (fcu). After surpassing this threshold, the curve ascends progressively until it reaches the peak value (fcu), with this ascending segment being regarded as a parabola. Following its optimum value, the stress–strain curve promptly experiences a decline, which can be represented by a straight line**.**

3.2.2. Steel (PSS and C-purlin)

C-purlins is isotropic material, thus, the elastic–isotropic option was selected to identify. It has Young's modulus of 210 MPa and its Poisson's ratio and yield strength are 0.3 and 492 MPa respectively, while the Peva 50 profiled steel sheeting (PSS) is produced by roll-forming a steel plate in a rolling mill. The material exhibits Young's modulus of 213 MPa, Poisson's ratio of 0.3, and yield strength of 434 MPa, in that order. Figure 7 shows the trilinear stress–strain model for the steel material which was adopted in the current study, where this model has been earlier suggested by (Byfield et al. 2005).

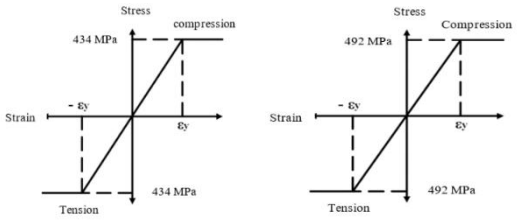

Fig. 7. Stress-strain curve for the profile steel sheet PSS and C-purlin.

4. Convergence Study

Finite Element (FE) analyses provide a wide range of convergence definitions, which include but are not limited to the convergence of the nonlinear solution procedure, mesh convergence, time integration accuracy, and contact control accuracy. As a result, decreasing the quantity of the number of elements while maintaining the precision of the outcomes is the most effective strategy.

Fig. 8 illustrates the convergence study on the relationship between the ultimate moment capacity (Mu) and the total number of elements used for the half FE models of the double filled, separate, and single specimens (DF, DS, S).

Table 2. Comparison between the results of the EX-tests and FE analysis for specimens.

No.	Specimens' designation	M_u (kNm)		
		M_{EX}	M_{FE}	M_{FE}/M_{EX}
1	CBPDS-DF	51.5	53.4	1.037
2	CBPDS-DS	46.5	49.0	1.053
3	CBPDS-S	31.9	33.8	1.060
			Mean value	1.050
			SD	0.012

5. Verifying the FE Models

The FE analysis results were validated using the experimental results of double, separate, and single specimens using the same material properties to verify the FE models.

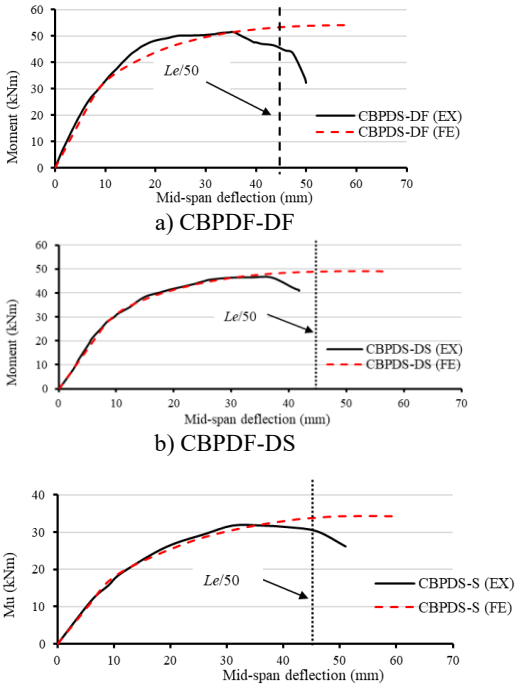

Fig. 8. Comparison between the experimental and FE results of the CBPDS (DF, DS, S).

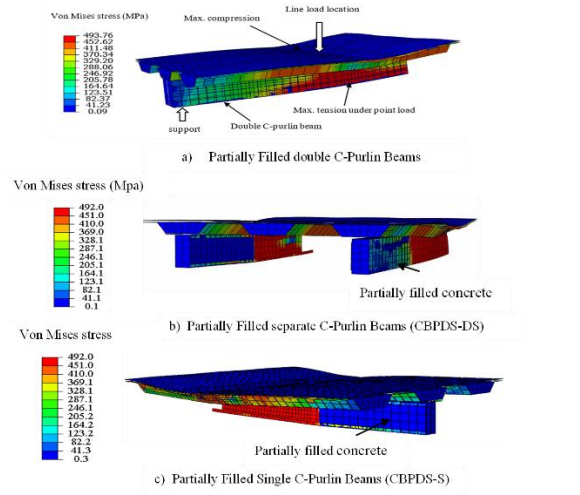

Fig. 9. 3D view of the CBPDS (DF, DS, S) model.

Table 2 presents the Mu values of the FE models subjected to two-point bending. The results were consistent with those of the experimental (EX) tests. Fig. 9 illustrates the load mid-span deflection curve of the double-filled, separate, and single specimens and the finite element model of the same specimens, and it is found that both are comparable in the elastic and plastic range with a minor discrepancy of 4%, 5.4%, and 6% respectively in the ultimate moment capacity. The comparison will be done in the matter of performance and the moment value at the displacement of Le/50 (45mm) for all samples [31]. Fig. 10 displays the Von Mises stress distribution of the double filled, separate, and single specimens, which shows that the maximum stress in the DB is around the load location which coincides with the failure mode of the experimental sample. And the maximum stress for the PSS lies and the C-purlin beam at the center under the load which also coincides with failure mode with an experimental specimen. Therefore, these models are considered accurate enough to predict the behaviour of the CBPDS (DF, DS, S) specimens.

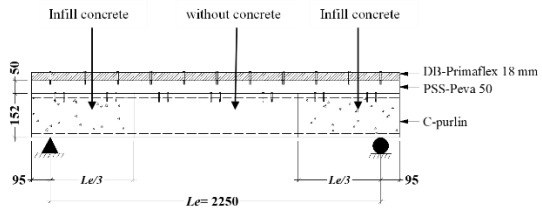

Fig. 10. Partially filled the C-purlin beams.

6. Parametric Studies

After verifying the FE models, three parametric studies were employed with a total number of FE models equal to 12 to deeply investigate the structural performance of the suggested CBPDS system in this research.

Table 3. Properties of the CBPDS-DF models with partially filled concrete.

Specimens Designation	C-purlin Thickness (mm)	PSS Thickness (mm)	DB Thickness (mm)	Partially filled (mm)	Ultimate Moment (kN.m)
CBPDS-DF-Le	**2**	**1**	**18**	**2250**	**53.4**
CBPDS-DF-Le/3	**2**	**1**	**18**	**750.0**	**38.5**
CBPDS-DF-Le/4	**2**	**1**	**18**	**562.5**	**28.8**
CBPDS-DF-Le/5	**2**	**1**	**18**	**450.0**	**27.8**

This parametric study aims to examine the effects of different partially filled concrete (Le, Le/3, Le/4, and Le/5 of C-purlin beam lengths) on the behaviour of the CBPDS system (see Fig.11). The comparison will be presented and discussed in three parts: the first part for the CBPDS-DF models, the second part for the CBPDS-DS models, and then for the CBPDS-S models, respectively.

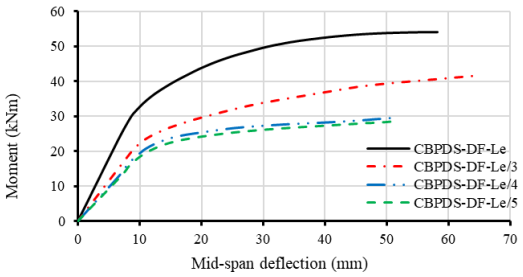

Fig. 11. Moment-deflection curves for the CBPDS-DF models with partially filled concrete.

6.1. Effect of partially filled double C-Purlin beams

Four FE models were prepared for CBPDS-DF as shown in Table 3, where each one has a double C-purlin face-to-face with different partial filling of the concrete (450, 562.5, 750, and 2250 mm). All of them have the same DB, PSS, and C-purlin. Also, it has the same screw spacing and boundary conditions.

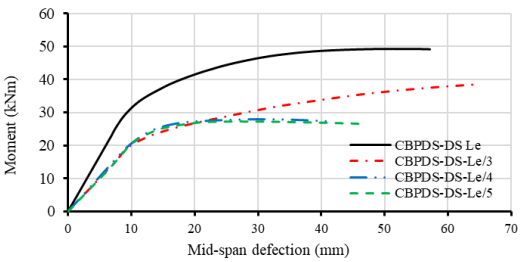

Fig. 12. Moment-deflection curves for the CBPDS-DS with partially filled concrete.

Table 4. Properties of the CBPDS-DS with partially filled concrete.

Specimens Designation	C-purlin Thickness (mm)	PSS Thickness (mm)	DB Thickness (mm)	Partially filled (mm)	Ultimate Moment (kN.m)
CBPDS-DS-Le	**2**	**1**	**18**	**2250**	**49.0**
CBPDS-DS-Le/3	**2**	**1**	**18**	**750.0**	**35.2**
CBPDS-DS-Le/4	**2**	**1**	**18**	**562.5**	**27.9**
CBPDS-DS-Le/5	**2**	**1**	**18**	**450.0**	**27.2**

Figure 12 shows that partially filling the C-purlin section significantly affects the CBPDS system. For the CBPDS-DF models, the specimen with a double filled C-purlins beam (Full infill) is considered a reference model (CBPDS-DF-Le). The moment capacity of this model is equal to 53.4 kN.m which was reduced to 38.5, 28.8, and 27.8 kN.m (-28%, -46%, and -48%) respectively, when the same models used the CBPDS-DF-Le/3, CBPDS-DF-Le/4, and CBPDS-DF-Le/5. Table 5.11 Properties of the CBPDS-DF models with partially filled concrete.

Table 5. Properties of the CBPDS-S models with partially filled concrete.

Specimens Designation	C-purlin Thickness (mm)	PSS Thickness (mm)	DB Thickness (mm)	Partially filled (mm)	Ultimate Moment (kN.m)
CBPDS-S-Le	**2**	**1**	**18**	**2250**	**33.8**
CBPDS-S-Le/3	**2**	**1**	**18**	**750.0**	**19.6**
CBPDS-S-Le/4	**2**	**1**	**18**	**562.5**	**16.2**
CBPDS-S-Le/5	**2**	**1**	**18**	**450.0**	**15.6**

6.2. Effect of partially filled separate C-Purlin beams

Four models were prepared for CBPDS-DS as shown in Table 4. All of them have the same DB, PSS, C-purlin, screw spacing, and the boundary conditions. However, each one has a double separate C-purlin with different partially filled with concrete (450, 562.5, 750, and 2250 mm). The results presented in Fig. 13 indicate that altering the various partially filled concrete components significantly impacts the CBPDS system, exhibiting behavior similar to that of the CBPDS-DF models. The specimen featuring double separate filled C-purlins beam (Fully filled) serves as the reference model for the CBPDS-DS models (CBPDS-DS-Le). The initial capacity of this model is 49 kN.m, which reduced to 35.2, 27.9, and 27.2 kN.m (-28.1%, -43%, and -44%) respectively, when employing the CBPDS-DS-Le/3, CBPDS-DS-Le/4, and CBPDS-DS-Le/5 models. Utilizing double separate C-purlins beams (model CBPDS-DS-Le/3) resulted in an approximate 8.6% reduction in the specimen's bending capacity compared to the double filled C-purlins beams (face-to-face connection) CBPDS-DF-Le/3, as the separate C-sections were unable to sufficiently confine the concrete core, in contrast to their closed tubular configuration.

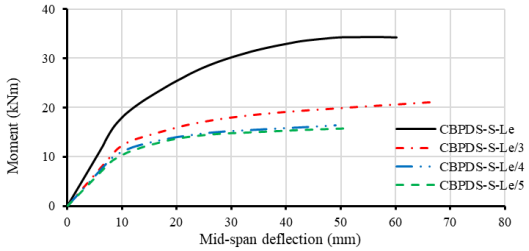

Fig. 13. Moment-deflection curves for the CBPDS-S models with partially filled concrete.

6.3. Effect of partially filled single C-Purlin beams

Four FE models were prepared for CBPDS-S as shown in Table 5, where each one has a single C-purlin with different partial filling of the concrete (450, 562.5, 750, and 2250 mm). All of them have the same DB, PSS, and C-purlin. Also, it has the same screw spacing and boundary conditions. The results presented in Fig. 14 have demonstrated that partially filling the concrete inside the C-purlin section has a significant effect on the CBPDS system, which is similar behaviour to CBPDS-DF and CBPDS-DS models. For the CBPDS-S models, the model with a single C-purlins beam (Full infill) is considered a reference model (CBPDS-S-Le). The moment capacity of this specimen is 33.8 kN.m which was decreased to 19.6, 16.2, and 15.6 kN.m (-42%, -45%, and -54%) respectively, when the same models used the CBPDS-S-Le/3, CBPDS-S-Le/4, and CBPDS-S-Le/5. Generally, regardless of the different configurations of the C-purlin, The C-purlin beam's ultimate moment capacity can be dramatically impacted by partially filling the concrete inside the beam section. In contrast, partially filled double separate C-purlin beams are more susceptible to local buckling and may exhibit a more brittle failure mode, particularly if the steel section is thin or slender. The ultimate moment capacity of the C-purlin beam is often less than that of a completely filled C-purlin beam when the beam is partially filled with concrete. This decrease happens because there is less concrete in the area that is only partially filled to help resist bending

forces, which in turn will accelerate its failure. Furthermore, a partial filling may also result in a reduced shear capacity, potentially influencing the overall structural performance.

7. Conclusion and Recommendations

- The four CBPDS-DF FE models show that partially filling the C-purlin section with concrete significantly affects structural performance. As concrete infill declines, beam moment capacity decreases significantly. The completely filled model (CBPDS-DF-Le) had the highest moment capacity of 53.4 kN.m, while the models with lower infill had 28%, 46%, and 48% reductions. Concrete infill is essential to the CBPDS-DF system's strength and stiffness.
- Like CBPDS-DF models, concrete infill greatly impacts moment capacity. The completely filled model (CBPDS-DS-Le) had the largest moment capacity of 49 kN.m, while models with lower infill had 28.1%, 43%, and 44% decreases. The study also found that double-separate C-purlins (CBPDS-DS-Le/3) have an 8.6% lower bending capability than face-to-face connected ones. In contrast to the closed tube-like design, which improves structural performance, individual C-sections cannot limit the concrete core.
- The four FE models for CBPDS-S show that partially filling the C-purlin section with concrete significantly affects structural performance, similar to the CBPDS-DF and CBPDS-DS models. Fully filled models (CBPDS-S-Le) had the highest moment capacity of 33.8 kN.m, while lower infill models had 42%, 45%, and 54% decreases. The study shows that partially filling the beam section with concrete reduces ultimate moment capacity regardless of C-purlin design. If the steel section is thin or slender, partially filled double separate C-purlin beams are inclined to local buckling and brittle failure. Reduced concrete infill reduces beam bending resistance, increasing structural failure. The impact of using recycled materials, effects of dry board (DB) thickness, profile steel sheet (PSS), and C-purlin thickness. could be studied in future studies.

8. Abbreviations

Cold-formed beam (CB), dry board (DB), Profile steel sheet (PSS), PSS slab covered with DB (PSSDB/PDS), ultimate bending moment capacity (flexural strength capacity; Mu), yield tensile strength of steel (fy), steel C-section thickness (t), effective length (Le).

References

[1] Wright, H.D.; Evans, H.R. A Folded Plate Method of Analysis for Profiled Steel Sheeting in Composite Floor Construction. Thin-Walled Struct. 1987, 5, 21–37, doi:10.1016/0263-8231(87)90014-0.

[2] Wright, H.D.; Evans, H.R.; Burt, C.A. Profiled Steel Sheet/Dry Boarding Composite Floors. Struct. Eng. Part A J. Inst. Struct. Eng. 1989, 67.

[3] Ahmed, E. Behavior of Profiled Steel Sheet Dry Board Folded Plate Structures. Unpubl. Dr. Philos. thesis, Univ. Kebangs. Malaysia, Selangor 1999.

[4] Wan Badaruzzaman, W.H.; Evans, H.R. Profiled Steel Sheeting Dry Board System as an Alternative to Traditional Forms of Construction. In Proceedings of the Proceedings of an International Conference on Advances in Strategic Technologies. UKM, Malaysia: Faculty of Engineering; 1995.

[5] Wan Badarllzzaman, W.H.; Ahmed, E.; Rashid ABSTRACf, K. Out-of Plane Bending Stiffness along the Major Axis of Proflled Steel Sheet Dryboard Composite Floor Panels. lurna! Kejuruter. 1996, 8, 79–95.

[6] Seraji, M.; Wan Badaruzzaman, W.H.; Osman, S.A. Membrane Action in Profiled Steel Sheeting Dry Board (PSSDB) Floor Slab System. J. Eng. Sci. Technol. 2013, 8, 57–68.

[7] Roslan, A.S.; Majid, M.A.; Jaini, Z.M.; Sutiman, N.A. Characterization of Bond-Slip Behaviour of the Profiled Steel Sheet Dry Board (PSSDB) Composite System Aina. Int. J. Integr. Eng. 2021, 13, 329–336.

[8] Zaid A. Al-Sudani , Fatimah De'nan , Ahmed W. Al-Zand, Noorhazlinda Abd Rahman, M.C.L. 2024. Flexural Performance of a New Composite Double PSSDB Slab System Filled with Recycled Concrete. Civil Engineering Journal 10(12). Civ. Eng. J. 2024, 10, doi:http://dx.doi.org/10.28991/CEJ-2024-010-12-03.

[9] Jaffar, M.I.; Badaruzzaman, W.H.W.; Baharom, S. Experimental Tests on Bending Behavior of Profiled Steel Sheeting Dry Board Composite Floor with Geopolymer Concrete Infill. Lat. Am. J. Solids Struct. 2016, 13, 272–295.

[10] Al-Shaikhli, M.S.; Wan Badaruzzaman, W.H.; Baharom, S.; Al-Zand, A.W. The Two-Way Flexural Performance of the PSSDB Floor System with Infill Material. J. Constr. Steel Res. 2017, 138, 79–92, doi:10.1016/j.jcsr.2017.06.039.

[11] Jaffar, M.I.; Wan Badaruzzaman, W.H.; Al Bakri Abdullah, M.M.; Abd Razak, R. Comparative Study Floor Flexural Behavior of Profiled Steel Sheeting Dry Board between Normal Concrete and Geopolymer Concrete In-Filled. Appl. Mech. Mater. 2015, 754–755, 364–368, doi:10.4028/www.scientific.net/amm.754-755.364.

[12] Fernando, P.L.N.; Jayasinghe, M.T.R.; Jayasinghe, C. Structural Feasibility of Expanded Polystyrene (EPS) Based Lightweight Concrete Sandwich Wall Panels.

Constr. Build. Mater. 2017, 139, 45–51, doi:10.1016/j.conbuildmat.2017.02.027.

[13] Jasim Hilo, S.; Wan Badaruzzaman, W.H.; Osman, S.A.; Al Zand, A.W. Axial Load Behavior of Acomposite Wall Strengthened with an Embedded Octagon Cold-Formed Steel. Appl. Mech. Mater. 2015, 754–755, 437–441, doi:10.4028/www.scientific.net/amm.754-755.437.

[14] Hilo, S.J.; Wan Badaruzzaman, W.H.; Osman, S.A.; Al Zand, A.W.; Samir, M.; Hasan, Q.A. A State-of-the-Art Review on Double-Skinned Composite Wall Systems. Thin-Walled Struct. 2015, 97, 74–100, doi:10.1016/j.tws.2015.09.007.

[15] Kim, H.-Y.; Jeong, Y.-J. Steel–Concrete Composite Bridge Deck Slab with Profiled Sheeting. J. Constr. Steel Res. 2009, 65, 1751–1762.

[16] Liu, J.; Ding, F.X.; Liu, X.M.; Yu, Z.W.; Tan, Z.; Huang, J.W. Flexural Capacity of Steel-Concrete Composite Beams under Hogging Moment. Adv. Civ. Eng. 2019, 2019, doi:10.1155/2019/3453274.

[17] Grover, K. Flexural Capacity of Composite Beams (Steel & Concrete) – A Review. IOSR J. Mech. Civ. Eng. 2016, 01, 66–72, doi:10.9790/1684-15010010166-72.

[18] He, Z.Q.; Ou, C.; Tian, F.; Liu, Z. Experimental Behavior of Steel-Concrete Composite Girders with Uhpc-Grout Strip Shear Connection. Buildings 2021, 11, doi:10.3390/buildings11050182.

[19] Liejy, M.C.; Al Zand, A.W.; Mutalib, A.A.; Alghaaeb, M.F.; Abdulhameed, A.A.; Al-Attar, A.A.; Tawfeeq, W.M.; Hilo, S.J. Flexural Performance of a Novel Steel Cold-Formed Beam–PSSDB Slab Composite System Filled with Concrete Material. Buildings 2023, 13, doi:10.3390/buildings13020432.

[20] Liejy, M.C.; Al Zand, A.W.; Mutalib, A.A.; Abdulhameed, A.A.; Kaish, A.B.M.A.; Tawfeeq, W.M.; Baharom, S.; Al-Attar, A.A.; Hanoon, A.N.; Yaseen, Z.M. Prediction of the Bending Strength of a Composite Steel Beam–Slab Member Filled with Recycled Concrete. Materials (Basel). 2023, 16.

[21] Seraji, M.; Badaruzzaman, W.H.W.; Osman, S.A. Experimental Study on the Compressive Membrane Action in Profiled Steel Sheet Dry Board (PSSDB) Floor System. Int. J. Adv. Sci. Eng. Inf. Technol. 2012, 2, 159–161.

[22] Jaffar, M.I.; Badaruzzaman, W.H.W.; Abdullah, M.M.A.B.; Baharom, S.; Wan Badaruzzaman, W.H.; Al Bakri, A.M.; Baharom, S. Experimental Test and Non-Linear Finite Element Modeling Prediction on Profiled Steel Sheeting Dry Board (PSSDB) with Geopolymer Concrete Infill. In Proceedings of the Key Engineering Materials; Trans Tech Publ, 2016; Vol. 673, pp. 75–81.

[23] Al Zand, A.W.; Hosseinpour, E.; Badaruzzaman, W.H.W.; Ali, M.M.; Yaseen, Z.M.; Hanoon, A.N. Performance of the Novel C-Purlin Tubular Beams Filled with Recycled-Lightweight Concrete Strengthened with CFRP Sheet. J. Build. Eng. 2021, 43, 102532, doi:10.1016/j.jobe.2021.102532.

[24] Lu, H.; Han, L.H.; Zhao, X.L. Analytical Behavior of Circular Concrete-Filled Thin-Walled Steel Tubes Subjected to Bending. Thin-Walled Struct. 2009, 47, 346–358, doi:10.1016/j.tws.2008.07.004.

[25] Moon, J.; Roeder, C.W.; Lehman, D.E.; Lee, H.E. Analytical Modeling of Bending of Circular Concrete-Filled Steel Tubes. Eng. Struct. 2012, 42, 349–361, doi:10.1016/j.engstruct.2012.04.028.

[26] Hilo, S.J.; Badaruzzaman, W.H.W.; Osman, S.A.; Al-zand, A.W. Thin-Walled Structures Structural Behavior of Composite Wall Systems Strengthened with Embedded Cold-Formed Steel Tube. Thin Walled Struct. 2016, 98, 607–616, doi:10.1016/j.tws.2015.10.028.

[27] Hognestad, H.E. A Study of Combined Bending and Axial Load in Reinforced Concrete Members; 1951;

[28] Bangash, M.Y.H. Concrete and Concrete Structures: Numerical Modelling and Applications; United Kingdom, 1989;

[29] Wang, T.; Hsu, T.T.C. Nonlinear Finite Element Analysis of Concrete Structures Using New Constitutive Models. Comput. Struct. 2001, 79, 2781–2791, doi:10.1016/S0045-7949(01)00157-2.

[30] Majewski, Sjph. The Mechanics of Structural Concrete in Terms of Elasto-Plasticity. Publ. House Silesian Univ. Technol. Gliwice 2003.

[31] Javed, M.F.; Ramli Sulong, N.H.; Memon, S.A.; Rehman, S.K.U.; Khan, N.B. Flexural Behaviour of Steel Hollow Sections Filled with Concrete That Contains OPBC as Coarse Aggregate. J. Constr. Steel Res. 2018, 148, 287–294, doi:10.1016/j.jcsr.2018.05.035.